An envelope model to describe the sensor dynamics of vibratory gyroscopes

An envelope model to describe the sensor dynamics of vibratory gyroscopes

Markus Egretzberger and Andreas Kugi

Automation and Control Institute, Vienna University of Technology, Austria

ABSTRACT

In this contribution, a method will be introduced to derive an envelope model for vibratory gyroscopes capturing the essential "slow" dynamics (envelope) of the system. The methodology will be exemplarily carried out for a capacitive gyroscope with electrostatic actuators and sensors. The resulting envelope model can be utilized for transient simulations with the advantage of a significantly increased simulation speed as well as for steady state simulations. Especially for the sensor design and optimization, where usually very complex mathematical models are used, efficient steady state simulations are of certain interest. Another great advantage of this approach is that the steady state solutions in terms of the envelope model are constant. Thus, for the controller design, a linearization of the nonlinear envelope model around the steady state solution yields a linear time-invariant system allowing for the application of the powerful methods known from linear control theory.

Keywords: MEMS gyroscopes, resonance structures, capacitive sensors and actuators, envelope model

1. INTRODUCTION

Vibratory micro electromechanical gyroscopes are typically driven by a primary oscillator. This primary oscillation is usually excited close to the resonance frequency in order to achieve maximum amplitudes. Similar to many electronic circuits, in particular in information technology, the wanted signal is modulated in a high-frequency carrier signal. Thus, the rate of change of the wanted signals is several orders of magnitude slower than the carrier frequency. In the case of the vibratory micro electromechanical gyroscopes under consideration an external angular rate causes a secondary oscillation with an amplitude proportional to the angular rate component about the sensitive axis exploiting the Coriolis effect. The output signal of the sensor (i.e., the angular rate) is obtained by an appropriate demodulation of the secondary oscillation signal. In order to provide a linear sensor behavior with maximum sensitivity the frequency and amplitude of the primary oscillation have to be controlled. Therefore, control circuits are used with a functionality similar to those of phase-locked loop and automatic gain-control circuits. Furthermore, micro electromechanical sensors are subject to large quadrature errors due to limitations in the fabrication process. These quadrature errors typically are due to a mechanical unbalance which causes a coupling between the primary and secondary oscillation even without an applied external angular rate. This quadrature signal can be separated from the angular rate signal after the demodulation of the secondary oscillation. In order to avoid a drift of the output signal, e.g., over the temperature, due to demodulation errors the mechanical unbalance has to be actively compensated. Therefore, an additional actuation of the secondary oscillator has to be provided such that a controller can be implemented to suppress the unwanted quadrature signal. In this context, many articles dealing with the control of vibratory gyroscopes can be found in the literature, see, e.g., Ref. 1–7. In addition to the above mentioned control tasks necessary for the basic operation of micro electromechanical gyroscopes, force-feedback control and frequency control of the secondary resonance frequency are often used to further enhance the sensor performance. All of the mentioned control loops have in common that the relevant closed-loop dynamics lie within the frequency range of the envelope of the signal rather than in the frequency range of the carrier signal itself. In particular in view of system analysis and controller design, this motivates to derive a more comprehensive mathematical model which solely captures the essential "slow" dynamics (envelope) of the system.

Further author information: (Send correspondence to Markus Egretzberger)
M.E.: E-mail: egretzberger@acin.tuwien.ac.at, Telephone: +43 1 58801 37626
A.K.: E-mail: kugi@acin.tuwien.ac.at, Telephone: +43 1 58801 37614

Post-print version of the article: M. Egretzberger and A. Kugi, "An envelope model to describe the sensor dynamics of vibratory gyroscopes", in *SPIE Europe: Microtechnologies for the New Millennium, Smart Sensors, Actuators, and MEMS IV*, Dresden, Germany, Apr. 2009.
DOI: 10.1117/12.821705

In this contribution, a method will be introduced to derive an envelope model for vibratory gyroscopes. The methodology will be exemplarily carried out for a capacitive micro electromechanical gyroscope. This paper is organized as follows. In Sec. 2 the specific capacitive gyroscope is discussed, which will serve as a practical example for the theory being presented. A mathematical model for the gyroscope under consideration is given as a starting point for the derivation of an envelope model in Sec. 3. In view of the sensor design and optimization, where usually very complex mathematical models (e.g., FEM models) are used, efficient steady state simulations are of certain interest. Therefore, Sec. 4 is focused on the calculation of the steady state response based on the envelope model. A typical example that will be illustrated is the problem of dimensioning the capacitive actuators for the compensation of the mechanical unbalance of the gyroscope. Additionally, the aim is to trim the resonance frequency of the secondary oscillation to a desired predefined value. For this, a procedure is presented for the calculation of the unbalance compensated and frequency trimmed steady state. Finally, Sec. 5 gives a short summary and an outlook to further research activities.

2. A CAPACITIVE GYROSCOPE

The micro electromechanical device that will be considered within this paper is a gyroscope consisting of a plane symmetric silicon structure operating with an in-plane primary mode, excited by capacitive comb actuators, and an out-of-plane secondary mode with capacitive parallel plate sensors. Most capacitive gyroscopes found in the literature are driven by electrostatic comb actuators bringing about the advantage of a high actuation force and little required space. They are found in linear oscillating as well as in rotating designs, see e.g., Ref. 6, 8–11 and Ref. 12, respectively. For the same reason the read-out of the secondary oscillation is preferably realized by means of comb sensors. In practice comb sensors can only be realized if the secondary mode is also an in-plane oscillation as it is the case for the designs presented in Ref. 8–11. If the secondary mode is an out-of-plane oscillation, parallel plate capacitors are utilized such that the movable electrode is part of the oscillating structure and the appropriate fixed electrode is mounted on the housing of the device, see e.g., Ref. 12. In Ref. 13 a capacitive gyroscope was developed with a linear oscillating primary mode driven by comb actuators in combination with a secondary mode that is oscillating out-of-plane.

Within the scope of this work several geometric designs deduced from the capacitive gyroscope presented in Ref. 13 have been studied. The increasing complexity of the sensor design and the large variety of design modifications have given rise to the development of a software tool for the automatic generation of an analytical mathematical model for this type of capacitive gyroscopes. This software tool is capable of reading slightly refined geometric design data provided by CAD tools and converts the geometric information of the structure into functional elements necessary for the physical modeling of the gyroscope. A data interface is provided for a program package developed for the commercial computer algebra program MAPLE, which allows for the analytical modeling of the gyroscope and the subsequent export of a suitable model for the numeric simulation environment MATLAB/SIMULINK. The software tool is described in more detail in Ref. 14 and will be utilized in the present work for the derivation of the mathematical model.

At this point, let us restrict ourselves to one specific design which is an enhanced version of the gyroscope presented in Ref. 13. This design is capable of both compensating the mechanical unbalance and tuning the eigenfrequency of the secondary mode. In this section, the working principle of the capacitive gyroscope will be explained and subsequently the appropriate mathematical model is derived.

2.1 Principle of operation

The capacitive gyroscope under consideration as depicted in Fig. 1 is an etched, plane silicon structure possessing two axes of symmetry. It consists of a rectangular fixed frame, which is rigidly mounted on the housing of the device, and two movable frames, one on the left and one on the right half of the sensor, which are flexibly connected to the fixed frame via elastic beams, the so-called drive beams. Moreover, two paddles are flexibly connected to each movable frame via torsion beams.

The comb actuators and comb sensors comprise electrodes residing on the fixed frame and their movable counterparts which are rigidly attached to the movable frames. The comb actuators allow for a harmonic excitation of the movable frames and the paddles in an anti-symmetric in-plane oscillation (primary mode). If an external angular rate is applied to the system the Coriolis force is coupling to the velocity of the movable

Post-print version of the article: M. Egretzberger and A. Kugi, "An envelope model to describe the sensor dynamics of vibratory gyroscopes", in *SPIE Europe: Microtechnologies for the New Millennium, Smart Sensors, Actuators, and MEMS IV*, Dresden, Germany, Apr. 2009.
DOI: 10.1117/12.821705
The content of this post-print version is identical to the published paper but without the publisher's final layout or copy editing.

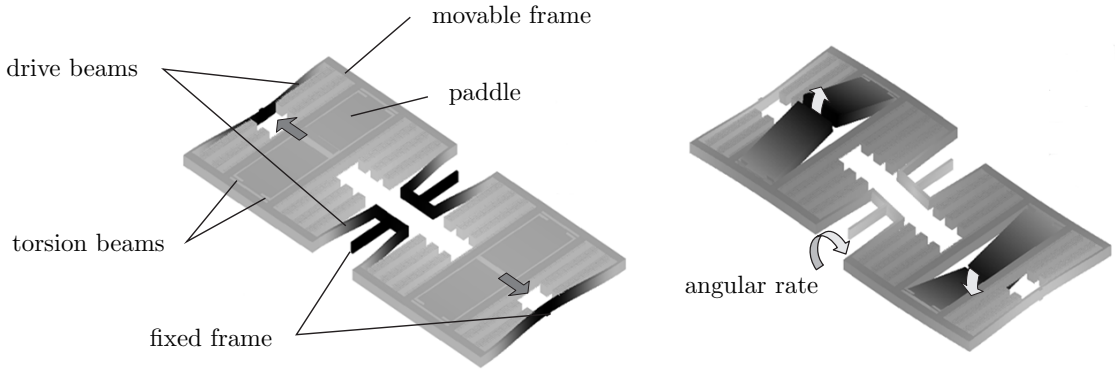

(a) Primary mode (b) Secondary mode

Figure 1. Schematic representation of the capacitive gyroscope (a) primary mode and (b) secondary mode.

frames and paddles causing an out-of-plane motion of these rigid body elements (secondary mode). The comb sensors provide the feedback signal for the amplitude control of the primary mode while the secondary mode is detected by means of four parallel plate capacitors with a fixed electrode placed above each paddle. Furthermore, there are additional capacitive parallel plate actuators, each of which consisting of several fixed electrodes placed above the movable frame and the paddles. The mechanical unbalance which is coupling between the primary and secondary mode is due to a distortion of the rectangular shaped cross sections of the beam elements, in particular at the drive meanders. In the mathematical model derived below this effect will be accounted for by means of beam elements with rhomboid cross sections characterized by the so-called side wall angle Γ, see Ref. 15. All electrostatic actuators are assumed to be voltage controlled with a desired input voltage, see e.g., Ref. 16. The electrostatic sensors are realized by means of a so-called charge amplifier circuit to convert the capacitance change into a proportional output voltage. These circuits are complemented by appropriate differential amplifiers in order to provide applicable output signals for the detection of the primary and secondary mode.

2.2 Mathematical model

As described in Subsec. 2.1 the micro electromechanical device is composed of several individual elements, i.e., the movable mechanical structure consisting of rigid elements (movable frame, paddle), elastic elements (beam structures) and the electrostatic actuators (comb and parallel plate capacitors). In a more general form, the capacitive gyroscope can be considered as a multi-body system made up of rigid and elastic bodies with external forces applied by the capacitive actuators. The equations of motion can be derived by means of Lagrange's formalism utilizing the software tool presented in Ref. 14. The resulting model is a system of non-linear ordinary differential equations of the form

$$\mathbf{M}(\mathbf{z})\,\ddot{\mathbf{z}} + \mathbf{C}(\mathbf{z},\dot{\mathbf{z}},\Omega)\,\dot{\mathbf{z}} + \mathbf{f}\big(\mathbf{z},\mathbf{u},\Omega,\dot{\Omega},\Gamma\big) = \mathbf{0} \tag{1a}$$

with the output

$$\mathbf{y} = \mathbf{h}(\mathbf{z}) \ , \tag{1b}$$

the vector of the generalized displacements $\mathbf{z}$, the externally applied angular rate Ω and the vector of the input voltages $\mathbf{u}$ and output voltages $\mathbf{y}$. Note that $\mathbf{M}(\mathbf{z})$ is the positive definite inertia matrix, $\mathbf{C}(\mathbf{z},\dot{\mathbf{z}},\Omega)$ is the Coriolis matrix and the side wall angle Γ represents the mechanical unbalance of the gyroscope. Since the displacements $\mathbf{z}$ are small the autonomous mechanical system with $\Omega = 0$ and $\mathbf{u} = \mathbf{0}$ can be linearized around the equilibrium point $\mathbf{z} = \dot{\mathbf{z}} = \mathbf{0}$ and the eigenmodes and eigenvectors of the (decoupled) mechanical structure with $\Gamma = 0$ can be calculated. The state transformation $\mathbf{z} = \mathbf{T}\,\mathbf{q}$ with the regular matrix $\mathbf{T}$ containing the eigenvectors of the linearized system substituted in (1) yields a modal model which allows for a systematic order reduction. So far the system has been considered as a conservative system, i.e., without dissipative terms. Within the scope of this contribution a modal damping model will be used by adding the dissipative term $-\mathbf{D}\,\dot{\mathbf{q}}$ with a diagonal matrix $\mathbf{D}$.

Post-print version of the article: M. Egretzberger and A. Kugi, "An envelope model to describe the sensor dynamics of vibratory gyroscopes", in *SPIE Europe: Microtechnologies for the New Millennium, Smart Sensors, Actuators, and MEMS IV*, Dresden, Germany, Apr. 2009.
DOI: 10.1117/12.821705

Due to the specific design of the gyroscope some further simplification can be made. The structure is optimized to yield a maximum Coriolis effect while at the same time suppressing the inertia and centrifugal terms due to the external angular rate. In view of these assumptions all non-linear terms of the mechanical subsystem are neglected except for the Coriolis terms stemming from the external angular rate. Then the transformed (modal) system can be written in the form

$$\frac{\mathrm{d}}{\mathrm{d}t}\begin{bmatrix}\mathbf{q}\\ \mathbf{v}\end{bmatrix} = \begin{bmatrix}\mathbf{0} & \mathbf{I}\\ -\tilde{\mathbf{K}}(\Gamma) & -\tilde{\mathbf{D}}(\Omega)\end{bmatrix}\begin{bmatrix}\mathbf{q}\\ \mathbf{v}\end{bmatrix} - \begin{bmatrix}\mathbf{0}\\ \tilde{\mathbf{f}}(\mathbf{q},\mathbf{u})\end{bmatrix} \tag{2a}$$

with the output

$$\mathbf{y} = \tilde{\mathbf{h}}(\mathbf{q}) \ , \tag{2b}$$

the vectors of the states $\mathbf{q}, \mathbf{v} \in \mathbb{R}^n$, the vector of the input voltages $\mathbf{u} \in \mathbb{R}^m$ and the output voltages $\mathbf{y} \in \mathbb{R}^p$. Thereby, $\tilde{\mathbf{K}}(\Gamma)$ denotes the stiffness matrix of the mechanical system, the matrix $\tilde{\mathbf{D}}(\Omega)$ contains the dissipative terms and the Coriolis terms due to the external angular rate Ω and the vector $\tilde{\mathbf{f}}(\mathbf{q},\mathbf{u})$ comprises the non-linear electromechanical coupling terms due to the capacitive actuation.

In the case of the capacitive gyroscope from Fig. 1 the input vector $\mathbf{u}$ consists of m input voltages, namely the drive voltage u_D at the comb actuators and $m-1$ different compensation voltages applied to the parallel plate actuators for suppressing the unbalance due to the side wall angle Γ, for force feedback control and for tuning the eigenfrequency of the secondary mode. The exact number of compensation voltages is not specified at this stage, since it varies for each specific design under consideration. For the further calculations a numerical model reduced to $n = 8$ modes will be used. Thereby, the fundamental modes of the gyroscope, i.e., the primary and secondary mode, coincide with the second and third eigenmode q_2 and q_3 of the eight modes model, respectively. The primary and secondary eigenfrequencies are denoted as ω_P and ω_S and the modal damping is described by the quality factors Q_P and Q_S. Finally, the output vector $\mathbf{y} = [\,y_P,\, y_S\,]^{\mathrm{T}}$ consists of the primary and secondary detection voltages y_P and y_S provided by the capacitive comb sensors and parallel plate sensors, respectively.

3. ENVELOPE MODEL

Now the system (2) is excited with the harmonic drive voltage u_D with the aim to operate at the eigenfrequency of the primary mode. In many cases the relevant dynamics lie within the frequency range of the envelope of the signal rather than in the frequency range of the harmonically oscillating signals itself. This leads to the idea of developing a model that is described by the Fourier coefficients of the appropriate harmonic signals, see, e.g., Ref. 17.

Starting from the general mathematical model (2) a Fourier transformation $\mathbf{q} = \mathbf{Q}^{\mathrm{T}}\mathbf{w}$, $\mathbf{v} = \mathbf{V}^{\mathrm{T}}\mathbf{w}$, $\mathbf{u} = \mathbf{U}^{\mathrm{T}}\mathbf{w}$ and $\mathbf{y} = \mathbf{Y}^{\mathrm{T}}\mathbf{w}$ is performed with the Fourier coefficient matrices $\mathbf{Q}, \mathbf{V} \in \mathbb{R}^{2r+1\times n}$, $\mathbf{U} \in \mathbb{R}^{2r+1\times m}$ and $\mathbf{Y} \in \mathbb{R}^{2r+1\times p}$ of the form

$$\mathbf{Q} = \begin{bmatrix} Q_{1,0} & \cdots & Q_{n,0}\\ Q_{1,S} & & Q_{n,S}\\ Q_{1,C} & & Q_{n,C}\\ \vdots & \ddots & \vdots\\ Q_{1,rS} & & Q_{n,rS}\\ Q_{1,rC} & \cdots & Q_{n,rC}\end{bmatrix},\ \mathbf{V} = \begin{bmatrix} V_{1,0} & \cdots & V_{n,0}\\ V_{1,S} & & V_{n,S}\\ V_{1,C} & & V_{n,C}\\ \vdots & \ddots & \vdots\\ V_{1,rS} & & V_{n,rS}\\ V_{1,rC} & \cdots & V_{n,rC}\end{bmatrix},\ \mathbf{U} = \begin{bmatrix} U_{1,0} & \cdots & U_{m,0}\\ U_{1,S} & & U_{m,S}\\ U_{1,C} & & U_{m,C}\\ \vdots & \ddots & \vdots\\ U_{1,rS} & & U_{m,rS}\\ U_{1,rC} & \cdots & U_{m,rC}\end{bmatrix},\ \mathbf{Y} = \begin{bmatrix} Y_{1,0} & \cdots & Y_{p,0}\\ Y_{1,S} & & Y_{p,S}\\ Y_{1,C} & & Y_{p,C}\\ \vdots & \ddots & \vdots\\ Y_{1,rS} & & Y_{p,rS}\\ Y_{1,rC} & \cdots & Y_{p,rC}\end{bmatrix} \tag{3}$$

and the Fourier basis vector $\mathbf{w} \in \mathbb{R}^{2r+1}$ of the form

$$\mathbf{w} = \begin{bmatrix} 1, & \sin(\varphi), & \cos(\varphi), & \ldots, & \sin(r\varphi), & \cos(r\varphi) \end{bmatrix}^{\mathrm{T}} .$$

with the phase φ. The Fourier basis vector $\mathbf{w}$ satisfies the differential equation $\dot{\mathbf{w}} = \boldsymbol{\Omega}\,\mathbf{w}$ with the phase velocity

Post-print version of the article: M. Egretzberger and A. Kugi, "An envelope model to describe the sensor dynamics of vibratory gyroscopes", in *SPIE Europe: Microtechnologies for the New Millennium, Smart Sensors, Actuators, and MEMS IV*, Dresden, Germany, Apr. 2009.
DOI: 10.1117/12.821705

matrix

$$\mathbf{\Omega} = \begin{bmatrix} 0 & 0 & 0 & \cdots & 0 & 0 \\ 0 & 0 & \omega & & 0 & 0 \\ 0 & -\omega & 0 & & 0 & 0 \\ \vdots & & & \ddots & & \vdots \\ 0 & 0 & 0 & & 0 & r\omega \\ 0 & 0 & 0 & \cdots & -r\omega & 0 \end{bmatrix}$$

and the phase velocity $\omega = \dot{\varphi}$ of the fundamental oscillation. If it is assumed that the non-linear terms in (2) can be written in the form $\tilde{\mathbf{f}}(\mathbf{q}, \mathbf{u}) = \tilde{\mathbf{F}}^{\mathrm{T}}(\mathbf{Q}, \mathbf{U})\,\mathbf{w}$ and $\tilde{\mathbf{h}}(\mathbf{q}) = \tilde{\mathbf{H}}^{\mathrm{T}}(\mathbf{Q})\,\mathbf{w}$, the above Fourier transform substituted in (2) yields the matrix-valued differential equations

$$\frac{\mathrm{d}}{\mathrm{d}t}\begin{bmatrix} \mathbf{Q}^{\mathrm{T}} \\ \mathbf{V}^{\mathrm{T}} \end{bmatrix} = \begin{bmatrix} \mathbf{0} & \mathbf{I} \\ -\tilde{\mathbf{K}}(\Gamma) & -\tilde{\mathbf{D}}(\Omega) \end{bmatrix}\begin{bmatrix} \mathbf{Q}^{\mathrm{T}} \\ \mathbf{V}^{\mathrm{T}} \end{bmatrix} - \begin{bmatrix} \mathbf{0} \\ \tilde{\mathbf{F}}^{\mathrm{T}}(\mathbf{Q}, \mathbf{U}) \end{bmatrix} - \begin{bmatrix} \mathbf{Q}^{\mathrm{T}} \\ \mathbf{V}^{\mathrm{T}} \end{bmatrix}\mathbf{\Omega} \tag{4a}$$

with the output

$$\mathbf{Y}^{\mathrm{T}} = \tilde{\mathbf{H}}^{\mathrm{T}}(\mathbf{Q})\ . \tag{4b}$$

Since in general the Fourier transform of the non-linear terms cannot be calculated analytically the discrete Fourier transform will be utilized similarly to the approach proposed in Ref. 18 for the computation of circuit waveform envelopes. For this, a discretization of one period $T = 2\pi/\omega$ of the fundamental oscillation with N equidistant time steps is performed. If the discretized state vectors $\mathbf{q}_k$ and input vectors $\mathbf{u}_k$ for the time steps $k = 1, \ldots, N$ are merged into a matrix $\hat{\mathbf{q}} = [\,\hat{\mathbf{q}}_1, \ldots, \hat{\mathbf{q}}_N\,]^{\mathrm{T}}$ and $\hat{\mathbf{u}} = [\,\hat{\mathbf{u}}_1, \ldots, \hat{\mathbf{u}}_N\,]^{\mathrm{T}}$, respectively, the inverse discrete Fourier transform with real coefficients directly relates $\hat{\mathbf{q}}$ and $\hat{\mathbf{u}}$ with $\mathbf{Q}$ and $\mathbf{U}$ in the form

$$\hat{\mathbf{q}} = \frac{1}{N}\mathbf{\Lambda}\,\mathbf{Q}\ , \quad \hat{\mathbf{u}} = \frac{1}{N}\mathbf{\Lambda}\,\mathbf{U}$$

with the transformation matrix

$$\mathbf{\Lambda} = \begin{bmatrix} 1 & 0 & 1 & \ldots & 0 & 1 \\ \vdots & & & \ddots & & \vdots \\ 1 & \sin\left(2\pi\frac{k-1}{N}\right) & \cos\left(2\pi\frac{k-1}{N}\right) & \ldots & \sin\left(2\pi r\frac{k-1}{N}\right) & \cos\left(2\pi r\frac{k-1}{N}\right) \\ \vdots & & & \ddots & & \vdots \\ 1 & \sin\left(2\pi\frac{N-1}{N}\right) & \cos\left(2\pi\frac{N-1}{N}\right) & \ldots & \sin\left(2\pi r\frac{N-1}{N}\right) & \cos\left(2\pi r\frac{N-1}{N}\right) \end{bmatrix}\ .$$

If $N > 2r$, i.e. the sampling theorem is satisfied, the transformation matrix $\mathbf{\Lambda}$ has $2r+1$ linearly independent rows. Now the non-linear terms in (2) can be calculated for every time step $k = 1, \ldots, N$ in the form $\hat{\mathbf{f}}_k = \tilde{\mathbf{f}}(\hat{\mathbf{q}}_k, \hat{\mathbf{u}}_k)$ and $\hat{\mathbf{h}}_k = \tilde{\mathbf{h}}(\hat{\mathbf{q}}_k)$. Again the vectors $\mathbf{f}_k$ and $\mathbf{h}_k$ are merged into a matrix $\hat{\mathbf{f}} = [\,\hat{\mathbf{f}}_1, \ldots, \hat{\mathbf{f}}_N\,]^{\mathrm{T}}$ and $\hat{\mathbf{h}} = [\,\hat{\mathbf{h}}_1, \ldots, \hat{\mathbf{h}}_N\,]^{\mathrm{T}}$, respectively. Then the inverse discrete Fourier transform with real coefficients

$$\hat{\mathbf{F}} = \mathbf{\Lambda}^{\mathrm{T}}\,\hat{\mathbf{f}}\ , \quad \hat{\mathbf{H}} = \mathbf{\Lambda}^{\mathrm{T}}\,\hat{\mathbf{h}}$$

finally yields an approximation for the Fourier transform of the non-linear terms $\tilde{\mathbf{F}}(\mathbf{Q}, \mathbf{U}) \simeq \hat{\mathbf{F}}$ and $\tilde{\mathbf{H}}(\mathbf{Q}) \simeq \hat{\mathbf{H}}$.

4. CALCULATION OF THE STEADY STATE RESPONSE

Now a typical objective is to calculate the steady state response of the system (2) due to a harmonic excitation by the input $\mathbf{u}_S = \mathbf{U}_S^{\mathrm{T}}\,\mathbf{w}$. In terms of the corresponding envelope model (4) this is equivalent to the problem of finding the equilibrium $\mathbf{Q}_S$, $\mathbf{V}_S$ of the system (4) for the constant input $\mathbf{U}_S$. Thus, the steady state can be calculated by setting the time derivatives at the left hand side of (4a) equal to zero, i.e. solving the matrix-valued algebraic equations

$$\mathbf{0} = \mathbf{V}_S^{\mathrm{T}} - \mathbf{Q}_S^{\mathrm{T}}\mathbf{\Omega}\ , \quad \mathbf{0} = -\tilde{\mathbf{K}}(\Gamma)\,\mathbf{Q}_S^{\mathrm{T}} - \tilde{\mathbf{D}}(\Omega)\,\mathbf{V}_S^{\mathrm{T}} - \tilde{\mathbf{F}}(\mathbf{Q}_S, \mathbf{U}_S) - \mathbf{V}_S^{\mathrm{T}}\,\mathbf{\Omega}\ . \tag{5}$$

Post-print version of the article: M. Egretzberger and A. Kugi, "An envelope model to describe the sensor dynamics of vibratory gyroscopes", in *SPIE Europe: Microtechnologies for the New Millennium, Smart Sensors, Actuators, and MEMS IV*, Dresden, Germany, Apr. 2009. DOI: 10.1117/12.821705

In the following this procedure is applied to several tasks in the optimization and design process of the capacitive gyroscope. The system is excited by the harmonic drive voltage $u_D = U_{D,0} + U_{D,C}\cos(\omega t)$ at the eigenfrequency of the primary mode $\omega = \omega_P$. Furthermore, let us assume that two voltages $U_{T,0}$ and $U_{C,0}$ are applied to suitably designed parallel plate actuators in order to serve as control inputs for the tuning of the eigenfrequency of the secondary mode and the unbalance control, respectively. The dimension of the Fourier basis is chosen as $r = 1$ and thus the Fourier coefficient matrix of the input voltages according to (3) can then be written in the form

$$\mathbf{U}_S = \begin{bmatrix} U_{D,0} & U_{T,0} \pm U_{C,0} & \dots & U_{T,0} \pm U_{C,0} \\ 0 & 0 & \dots & 0 \\ U_{D,C} & 0 & \dots & 0 \end{bmatrix} .$$

If no external angular rate Ω is applied to the gyroscope and no mechanical unbalance is present the primary mode is fully decoupled from the residual system. In this case the primary mode turns out to behave like a weakly damped second order system that is harmonically excited close to the resonance frequency, thus yielding a large Fourier coefficient $Q_{2,S}$ while the Fourier coefficient $Q_{2,C}$ is vanishing. This effect is exploited within the control design of the primary mode in order to achieve the maximum sensitivity. In general, however, the system responds in steady state to a constant external angular rate Ω and/or a constant side wall angle Γ in the form

$$\mathbf{Q}_S = \begin{bmatrix} Q_{1,0} & Q_{2,0} & Q_{3,0} & Q_{4,0} & 0 & 0 & Q_{7,0} & Q_{8,0} \\ 0 & Q_{2,S} & Q_{3,S} & 0 & 0 & 0 & Q_{7,S} & 0 \\ 0 & Q_{2,C} & Q_{3,C} & 0 & 0 & 0 & Q_{7,C} & 0 \end{bmatrix} , \quad \mathbf{Y}_S = \begin{bmatrix} Y_{P,0} & Y_{S,0} \\ Y_{P,S} & Y_{S,S} \\ Y_{P,C} & Y_{S,C} \end{bmatrix} .$$

The only harmonically excited modes are the 2nd and 3rd eigenmodes (primary and secondary mode) as well as the 7th eigenmode. All other modes are either not or only stationary excited. The only relevant output signals are the harmonic components as due to the high-pass characteristics of the charge amplifiers the dc-components $Y_{P,0}$ and $Y_{S,0}$ are suppressed in the stationary output signal.

Now, in the following subsection the normal operation of the gyroscope shall be investigated in terms of the response to an external angular rate Ω and a mechanical unbalance due to a side wall angle Γ. For the subsequent numerical calculations a discretization of $N = 10$ for the approximation of the Fourier transforms of the non-linear terms is chosen.

4.1 Normal mode of operation

Let us consider a specific actuation of the parallel plate actuators with the constant voltages $U_{T,0} = 9\,\mathrm{V}$ and $U_{C,0} = 0\,\mathrm{V}$. Now the steady state response of the gyroscope is calculated (a) due to an external angular rate Ω and (b) due to a side wall angle Γ. Figure 2 illustrates the corresponding Fourier coefficients of the output signal $Y_{S,S}$ and $Y_{S,C}$ normalized to the response at $\Omega = 100\,^\circ/s$. Thereby, the range of the side wall angle Γ in Fig. 2(b) is chosen such that the normalized steady state response of the coefficient $Y_{S,S}$ for $\pm\Gamma_{100}$ is ∓ 1. Now it can be seen from Fig. 2(a) and 2(b) that within the plotted range the coefficients $Y_{S,C}$ and $Y_{S,S}$ are varying linearly with the angular rate and the side wall angle, respectively. The associated phasor diagram of the two coefficients $Y_{S,C}$ and $Y_{S,S}$, see Fig. 2(c), reveals a phase shift of $-90°$ between the output signal due to the angular rate and the output signal due to the side wall angle. This gives rise to the definition of the so-called normalized unbalance $\tilde{\Gamma} = \alpha\,\Gamma$ such that the magnitude $\sqrt{Y_{S,S}^2 + Y_{S,C}^2}$ of the output signal y_S due to an external angular rate of $1\,^\circ/\mathrm{s}$ and due to a normalized unbalance of $1\,^\circ/\mathrm{s}$ are equivalent. Furthermore, it can be observed that the unwanted unbalance signal can be separated from the angular rate signal by a proper demodulation of the output voltage y_S with two orthogonal reference signals. For a detailed treatise on the unbalance effects of micro electromechanical gyroscopes, see, e.g., Ref. 7.

The next subsection is concerned with the behavior of the gyroscope due to a mechanical unbalance $\tilde{\Gamma}$ and certain applied voltages $U_{T,0}$ and $U_{C,0}$ for the tuning of the eigenfrequency of the secondary mode and the unbalance control. For this, let us assume that no external angular rate Ω is applied to the gyroscope.

Post-print version of the article: M. Egretzberger and A. Kugi, "An envelope model to describe the sensor dynamics of vibratory gyroscopes", in *SPIE Europe: Microtechnologies for the New Millennium, Smart Sensors, Actuators, and MEMS IV*, Dresden, Germany, Apr. 2009.
DOI: 10.1117/12.821705

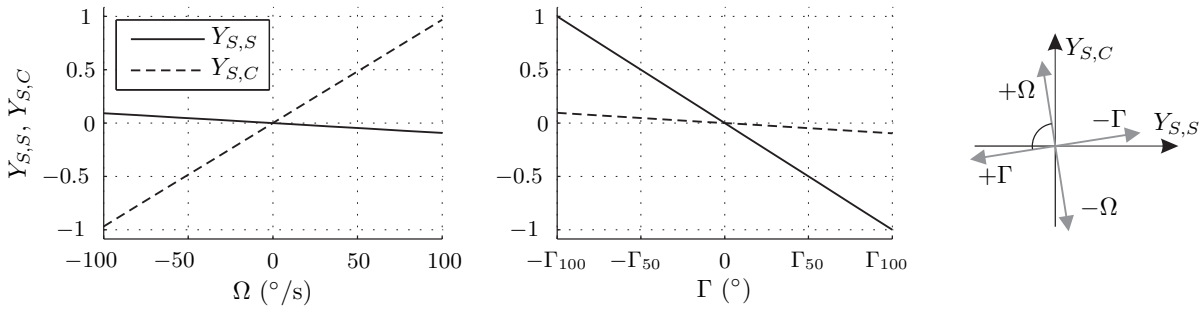

(a) response to external angular rate (b) response to side wall angle (c) phasor diagram

Figure 2. Steady state response of the system in terms of the Fourier coefficients $Y_{S,S}$ and $Y_{S,C}$ normalized to the response at $\Omega = 100\,°/s$ (a) due to an external angular rate Ω and (b) due to a side wall angle Γ with the appropriate phasor diagram (c).

4.2 Unbalance control and frequency tuning

Consider a gyroscope with a normalized unbalance of $\tilde{\Gamma} = 250\,°/\mathrm{s}$ where the applied voltages $U_{T,0}$ and $U_{C,0}$ are varied. Figure 3(a) illustrates the characteristics of the Fourier coefficients $Y_{S,S}$ and $Y_{S,C}$ in steady state over the range of the voltages $U_{T,0} = 3\,\mathrm{V} \ldots 9\,\mathrm{V}$ and $U_{C,0} = -3\,\mathrm{V} \ldots 3\,\mathrm{V}$, respectively. Again the coefficients $Y_{S,S}$ and $Y_{S,C}$ are normalized to the response due to $\tilde{\Gamma} = 100\,°/s$ at $U_{T,0} = 9\,\mathrm{V}$ and $U_{T,0} = 0$, cf. Fig. 2. Now a strongly non-linear characteristics of the coefficients $Y_{S,S}$ and $Y_{S,C}$ can be observed from Fig. 3(a). A

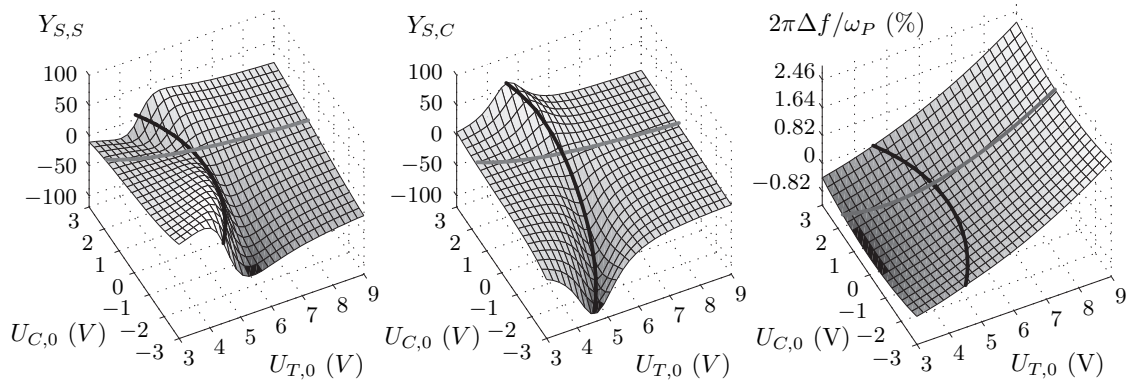

(a) components of the output voltage $Y_{S,S}$ and $Y_{S,C}$ (b) frequency difference Δf

Figure 3. Characteristics of system quantities in the steady state over the voltages $U_{T,0}$ and $U_{C,0}$ (a) in terms of the output components $Y_{S,S}$ and $Y_{S,C}$ normalized to the response due to $\tilde{\Gamma} = 100\,°/s$ at $U_{T,0} = 9\,\mathrm{V}$ and $U_{T,0} = 0$, cf. Fig. 2, and (b) in terms of the difference Δf between the eigenfrequencies of the primary and the secondary mode.

closer look reveals that both coefficients $Y_{S,S}$ and $Y_{S,C}$ can be suppressed along one characteristic line of voltage couples $U_{T,0}$ and $U_{C,0}$ marked in gray. The steady state obtained by applying the voltages $U_{T,0}$ and $U_{C,0}$ along this characteristic gray line will be referred to as the unbalance compensated state. Another characteristic line of voltage couples highlighted in black can be found where the component $Y_{S,S}$ is identically zero and at the same time the component $Y_{S,C}$ is extremal w.r.t. $U_{T,0}$. A different interpretation of this characteristic line can be found if the eigenfrequencies of the linearized system are considered. Therefore, the system (4a) is linearized around the equilibrium point $\mathbf{Q}_S$, $\mathbf{V}_S$ and $\mathbf{U}_S$ according to (5) and the eigenfrequencies of the linearized decoupled system with $\Gamma = 0$ are calculated. Figure 3(b) illustrates the distribution of the difference Δf between the eigenfrequencies of the primary and the secondary mode over the voltages $U_{T,0}$ and $U_{C,0}$. Again the two characteristic lines of voltage couples are plotted in Fig. 3(b). Now it can be seen that the black line exactly corresponds to a zero frequency difference between the primary and secondary mode, i.e. $\Delta f = 0$.

Post-print version of the article: M. Egretzberger and A. Kugi, "An envelope model to describe the sensor dynamics of vibratory gyroscopes", in *SPIE Europe: Microtechnologies for the New Millennium, Smart Sensors, Actuators, and MEMS IV*, Dresden, Germany, Apr. 2009.
DOI: 10.1117/12.821705

Consequentially, the steady state obtained by applying the voltages $U_{T,0}$ and $U_{C,0}$ along this characteristic black line will be referred to as the matched-mode state. The sensitivity of the gyroscope due to the external angular rate as well as the side wall angle is a maximum in this matched-mode state.

In the previous considerations it has been be shown how the unbalance and the eigenfrequencies of the linearized system, in particular the secondary eigenfrequency, can be affected by the voltages $U_{T,0}$ and $U_{C,0}$. Especially during the design process of capacitive gyroscopes, however, the inverse problem of calculating the necessary voltages $U_{T,0}$ and $U_{C,0}$ in order to achieve an unbalance compensated steady state where the frequency difference Δf becomes a desired predefined value is of certain interest. Exemplarily, the solution for the inverse problem has been carried out for the capacitive gyroscope under consideration yielding the necessary voltage couples $U_{T,0}$ and $U_{C,0}$ for the unbalance compensated and frequency trimmed steady state. The corresponding voltages $U_{T,0}$ and $U_{C,0}$ are plotted in Fig. 4 over the normalized unbalance $\tilde{\Gamma}$ for a range of the desired frequency difference $2\pi\Delta f/\omega_P$ from $-1.025\,\%$ to $4.1\,\%$. Due to the quadratic input non-linearity of the capacitive actuators

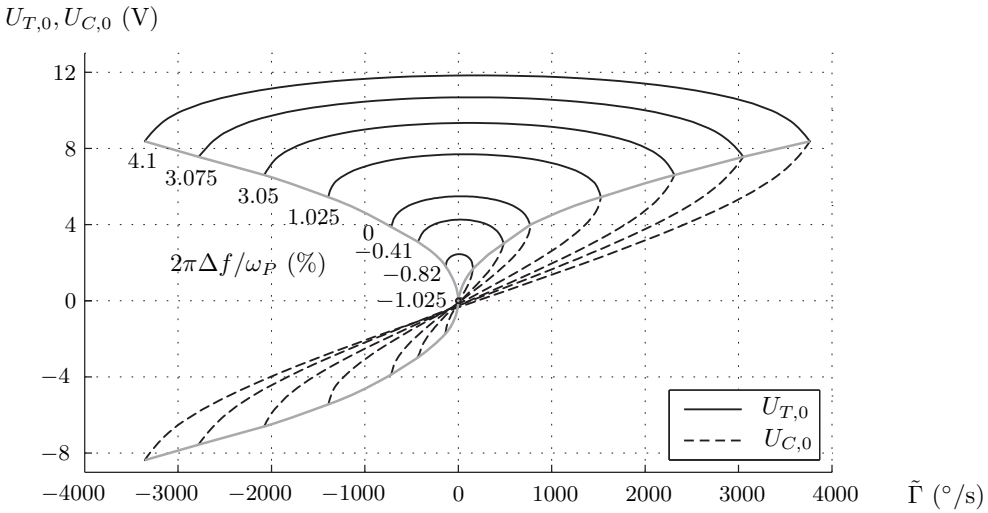

Figure 4. Necessary voltage couples $U_{T,0}$ and $U_{C,0}$ over the normalized unbalance $\tilde{\Gamma}$ for desired frequency differences Δf.

the unbalance compensation and the frequency trimming are subject to physical constraints. The gray line in Fig. 4 indicates the maximum and minimum possible normalized unbalance that can be compensated for the desired frequency difference.

5. SUMMARY AND OUTLOOK

The presented work provides a novel approach for the modeling, simulation and optimization of oscillating micro electromechanical devices in particular of vibratory MEMS gyroscopes. The methodology has been described exemplarily for a capacitive gyroscope. The advantages of the proposed approach for the steady state analysis have been outlined in detail. In this context, the normal mode of operation, i.e. the response to an external angular rate as well as to the disturbance stemming from a mechanical unbalance, was considered. Finally, the problem of systematically dimensioning the actuators for the compensation of the unbalance and the trimming of the secondary resonance frequency has been illustrated.

Beyond the discussed steady state applications the envelope model can also serve as a numerical model for transient simulations with the advantage of a drastically increased simulation speed. Furthermore, this modelling approach allows for a systematic controller design on the basis of the "slow" system dynamics provided by the envelope model. For this purpose, however, it is reasonable to make some more efforts in order reduction and further algebraic simplifications of the envelope model.

Post-print version of the article: M. Egretzberger and A. Kugi, "An envelope model to describe the sensor dynamics of vibratory gyroscopes", in *SPIE Europe: Microtechnologies for the New Millennium, Smart Sensors, Actuators, and MEMS IV*, Dresden, Germany, Apr. 2009. DOI: 10.1117/12.821705
The content of this post-print version is identical to the published paper but without the publisher's final layout or copy editing.

ACKNOWLEDGMENTS

This work was funded by the German BMBF as part of the EURIPIDES project RESTLES (project no. V3EUR015).

REFERENCES

[1] Bernstein, J., Cho, S., King, A. T., Kourepenis, A., Maciel, P., and Weinberg, M., "A micromachincd comb-drive tuning fork rate gyroscopce," in [*Proceedings MEMS*], 143–148 (1993).

[2] Maenaka, K., Fujita, T., Konishi, Y., and Maeda, M., "Analysis of a highly sensitive silicon gyroscope with cantilever beam as vibrating mass," *Sensors and Actuators A* **54**, 568–573 (1996).

[3] Kuisma, H., Ryhänen, T., Lahdenperä, J., Punkka, E., Routsalainen, S., Silanpää, T., and Seppä, H., "A bulk micromachined angular rate sensor," in [*The 9th Int. Conf. on Solid-State Sensors, Actuators and Microsystems, Transducers '97*], 875–878 (1997).

[4] Sassen, S., Voss, R., Schalk, J., Stenzel, E., Gleissner, T., Gruenberger, R., Neubauer, F., Ficker, W., Kupke, W., Bauer, K., and Rose, M., "Tuning fork silicon angular rate sensor with enhanced performance for automotive applications," *Sensors and Actuators A* **83**, 80–84 (2000).

[5] Loveday, P. W. and Rogers, C. A., "The influence of control system design on the performance of vibratory gyroscopes," *Journal of Sound and Vibration* **255**, 417–432 (2002).

[6] Bhave, S. A., Seeger, J. I., Jiang, X., Boser, B. E., Howe, R. T., and Yasaitis, J., "An integrated vertical-drive, in-plane-sense microgyroscope," in [*Digest of Technical Papers of the 12th International Conference on Solid-State Sensors, Actuators and Microsystems, Transducers '03*], 171–174 (2003).

[7] Günthner, S., Egretzberger, M., Kugi, A., Kapser, A., Hartmann, B., Schmid, U., and Seidl, H., "Compensation of parasitic effects for a silicon tuning fork gyroscope," *IEEE Sensors Journal* **6**, 596–604 (2006).

[8] Alper, S. and Akin, T., "A symmetric surface micromachined gyroscope with decoupled oscillation modes," in [*The 11th International Conference on Solid-State Sensors and Actuators, Transducers '01, Eurosensors XV*], 456–459 (2001).

[9] Braxmaier, M., Gaißer, A., Link, T., Schumacher, A., Simon, I., Frech, J., Sandmaier, H., and Lang, W., "Cross-coupling of the oscillation modes of vibratory gyroscopes," in [*Digest of Technical Papers of the 12th International Conference on Solid-State Sensors, Actuators and Microsystems, Transducers '03*], 167–170 (2003).

[10] Piyabongkarn, D., Rajamani, R., and Greminger, M., "The development of a MEMS gyroscope for absolute angle measurement," *IEEE Transactions on Control Systems Technology* **13**, 185–195 (2005).

[11] Seshia, A. A., Howe, R. T., and Montaguet, S., "An integrated microelectromechanical resonant output gyroscope," in [*The Fifteenth IEEE International Conference on Micro Electro Mechanical Systems*], (2002).

[12] Juneau, T., Pisano, A. P., and Smith, J. H., "Dual axis operation of a micromachined rate gyroscope," in [*The 9th International Conference on Solid-State Sensors, Actuators and Microsystems, Transducers '97*], **2**, 883–886 (1997).

[13] Günthner, S., "Entwurf und Charakterisierung von mikromechanischen Drehratensensoren in Silizium," in [*Aktuelle Berichte aus der Mikrosystemtechnik*], Shaker Verlag (2006).

[14] Mair, F., Egretzberger, M., and Kugi, A., "A tool for the automatic modeling of capacitive MEMS gyroscopes," in [*Proceedings of the 6th Vienna International Conference on Mathematical Modelling*], (2009).

[15] Merz, P., Pilz, W., Senger, F., Reimer, K., Grouchko, M., Pandhumsoporn, T., Bosch, W., Cofer, A., and Lassig, S., "Impact of Si DRIE on vibratory MEMS gyroscope performance," in [*The 14th International Conference on Solid-State Sensors, Actuators and Microsystems, Transducers & Eurosensors '07*], 1187–1190 (2007).

[16] Seeger, J. I. and Boser, B. E., "Charge control of parallel-plate, electrostatic actuators and the tip-in instability," *Journal of Microelectromechanical Systems* **12**, 656–671 (2003).

[17] Caliskan, V. A., Verghese, G. C., and Stankovic, A. M., "Multi-frequency averaging of DC/DC converters," in [*IEEE Workshop on Computers in Power Electronics*], 113–119 (1996).

[18] Feldman, P. and Roychowdhury, J., "Computation of circuit waveform envelopes using an effcient, matrix-decomposed harmonic balance algorithm," in [*Digest of Technical Papers of the ICCAD, IEEE/ACM International Conference*], 295–300 (1996).

Post-print version of the article: M. Egretzberger and A. Kugi, "An envelope model to describe the sensor dynamics of vibratory gyroscopes", in *SPIE Europe: Microtechnologies for the New Millennium, Smart Sensors, Actuators, and MEMS IV*, Dresden, Germany, Apr. 2009. DOI: 10.1117/12.821705